

Improved sensing using simultaneous deep UV Raman and fluorescence detection - II

W. F. Hug^{*a}, R. Bhartia^b, K. Sijapati^a, L. W. Beegle^b, and R.D. Reid^a

^a Photon Systems, Inc., 1512 Industrial Park St., Covina, CA 91722

^b Jet Propulsion Laboratory/Caltech, 4800 Oak Grove Dr., Pasadena, CA 91109

Abstract

Photon Systems in collaboration with JPL is continuing development of a new technology robot-mounted or hand-held sensor for reagentless, short-range, standoff detection and identification of trace levels chemical, biological, and explosive (CBE) materials on surfaces. This deep ultraviolet CBE sensor is the result of Army STTR and DTRA programs. The evolving 10 to 15 lb, 20 W, sensor can discriminate CBE from background clutter materials using a fusion of deep UV excited resonance Raman (RR) and laser induced native fluorescence (LINF) emissions collected in less than 1 ms. RR is a method that provides information about molecular bonds, while LINF spectroscopy is a much more sensitive method that provides information regarding the electronic configuration of target molecules.

Standoff excitation of suspicious packages, vehicles, persons, and other objects that may contain hazardous materials is accomplished using excitation in the deep UV where there are four main advantages compared to near-UV, visible or near-IR counterparts. 1) Excited between 220 and 250 nm, Raman emission occurs within a fluorescence-free region of the spectrum, eliminating obscuration of weak Raman signals by fluorescence from target or surrounding materials. 2) Because Raman and fluorescence occupy separate spectral regions, detection can be done simultaneously, providing an orthogonal set of information to improve both sensitivity and lower false alarm rates. 3) Rayleigh law and resonance effects increase Raman signal strength and sensitivity of detection. 4) Penetration depth into target in the deep UV is short, providing spatial/spectral separation of a target material from its background or substrate. 5) Detection in the deep UV eliminates ambient light background and enables daylight detection.

Keywords: deep UV Raman & native fluorescence; chemical, biological, and explosives detection and classification

1. INTRODUCTION

The goal of this paper is to demonstrate the advantages of employing a fused combination of Raman and fluorescence spectroscopy conducted in the deep UV to increase the probability of detection and reduce the probability of false detections compared to other miniature sensor methods. This paper is an extension of a prior paper [1]: *Bhartia, R., W. F. Hug, and R.D. Reid, "Improved sensing using simultaneous deep UV Raman and fluorescence detection", SPIE Security & Defense, Vol. 8358, No. 46, April 26, 2012*. This paper focuses on the advancements since this 2012 paper.

The new sensors under development are called targeted ultraviolet chemical, biological, and explosives (TUCBE) sensors. These new sensors are designed for operation on small military robots or as a hand-held sensor. The present TUCBE 4.5 sensor is nominally 15 lbs in weight and consumes less than 20 W from a battery or robot power source. Next generation sensors weigh about 8 lbs. Similar sensors with the same key components have been rated independently by the U.S. Army and NASA at technical readiness level (TRL) of 5.0+ in 2006. Versions of this sensor have been deployed on many expeditions to Antarctica, the Arctic, and the deep Ocean. In addition, they have been tested against a variety of chemical and explosives materials by Army/ECBC and NAVEODTECHDIV. They are being proposed for a space science mission to Mars as a 2020 Rover arm mounted instrument operating in very hostile conditions. This sensor uses a combination of resonance Raman (RR) and laser induced native fluorescence (LINF) spectroscopic methods using a laser emitting at 248.6 nm.

2. DEEP UV RAMAN AND LASER INDUCED NATIVE FLUORESCENCE

An example of the major advantage of operation in the deep UV is illustrated below in Fig. 1, where the combined Raman and fluorescence spectra of urea are shown, with the Raman spectral features occurring at wavelengths below

fluorescence emissions from trace organic contamination in the urea sample. Tyrosine and tryptophan are indicated as potential trace contaminants in what should be non-fluorescent urea. Asher [2] [3] showed that natural materials did not fluoresce below a wavelength about 270nm, independent of the excitation wavelength. This was further proven in many subsequent publications such as Nelson[4], Sparrow[5], Wu[6], and many others. When excitation occurs below about 250nm, a fluorescence-free region exists above the laser wavelength in which to observe Raman spectra. This is not the case for lasers that provide excitation at longer wavelengths, although excitation above 1 um produces reduced fluorescence backgrounds, but also produces very poor sensitivity. In the case of deep UV excitation, fluorescence is beneficial since it adds information to assist in sample identification.

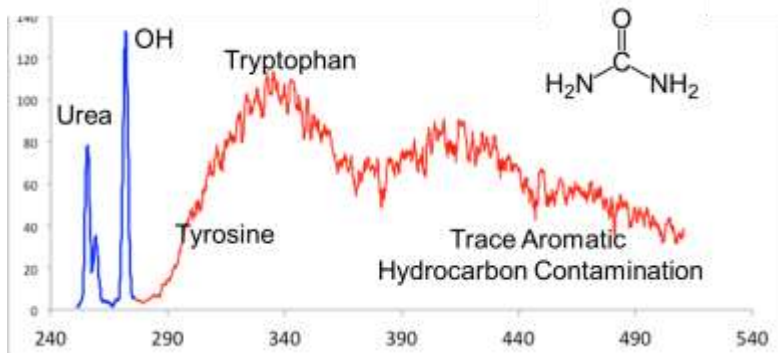


Figure 1. Simultaneous detection of Raman & fluorescence emissions from urea

Figure 2 further illustrates this with an example in Fig. 2A comparing the Raman spectra of crude oil excited both at 248 nm and 532 nm, and Chemical G agents excited at 248 nm and 262 nm, showing the sensitivity of excitation wavelength to obscuration of the Raman emissions.

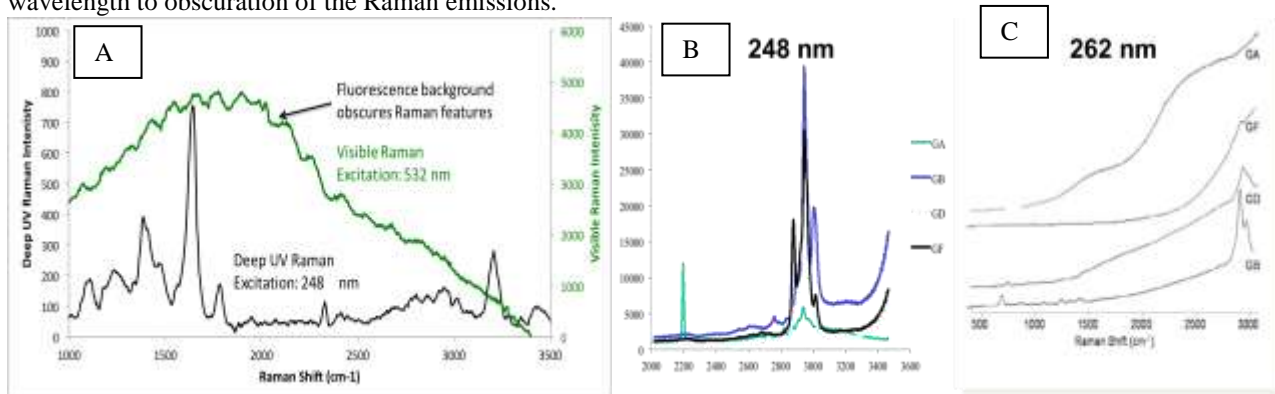


Figure 2. A) Raman spectra of crude oil with 248 nm & 532 nm excitation; B) Raman spectra of G-Agents with excitation at 248 nm [7]; and C) Raman spectra of G-Agents with 262 nm [7].

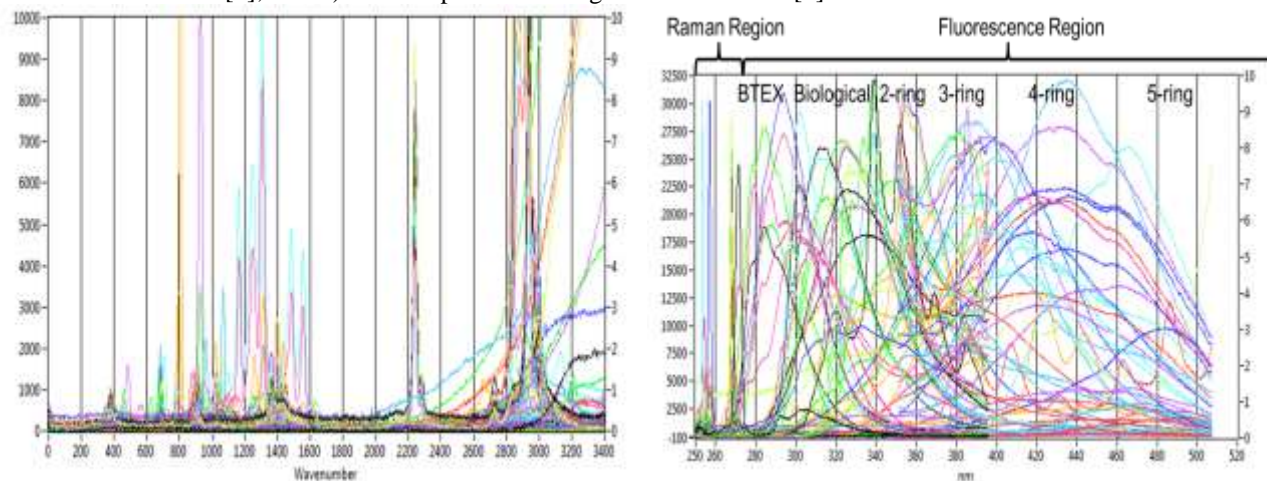


Figure 3. Excitation is at 248 nm. A) Raman spectra of 52 compounds; B) combined Raman & fluorescence spectra of same 52 compounds. *These spectra are raw, without any background subtraction or compensation and further illustrate the lack of fluorescence background for the vast majority of Raman spectra.* Also illustrated are the wealth of spectral variability and chemical information contained in the fluorescence spectra.

3. COMBINING RAMAN & FLUORESCENCE

An illustration of the importance of combining or fusing Raman and fluorescence information from targets is shown below in Fig. 4. Next to Rayleigh scattering, which contains relatively little information about a target, fluorescence and phosphorescence are the most efficient emitters from most target materials, providing the ability to detect and differentiate materials at much longer standoff distances and lower concentrations than Raman emissions. However, not all materials fluoresce or phosphoresce very well. It is a common misconception that fluorescence is not a very informative method since the fluorescence from different material cannot be distinguished, however as demonstrated in 2006 - 2008, excitation in the deep UV provides a unique differentiability [8-10]. Because of the efficiency of fluorescence from either target materials or their substrate or surrounding materials, weak Raman emissions are often masked unless excitation occurs below 250 nm. Separation of Raman and fluorescence emissions bands is essential even for weakly fluorescent materials or substrates. Even weakly fluorescent materials are still strong emitters compared to Raman. This is illustrated in Fig. 1. It is conversely true that strong water or CH Raman bands can also alter fluorescent emission spectra to lead to inaccurate conclusions unless these two spectral regions are separated. Materials that exhibit detectable Raman and fluorescence emissions include ammonium nitrates and nitrites, ketones, aldehydes, sulfuric acid, as well as explosive materials such as C4, Semtex, and ANFO's. Materials for which Raman is the only form of spectroscopic information includes water and non-aromatic amino acids, alcohols, and aliphatics. In Fig. 4, some materials, including DNA/RNA, explosive active ingredients and many chemical agents, strongly absorb both excitation and emission energy. These are among the most difficult materials to detect and are highlighted later in this paper.

Raman Active		Weak Fluorescence	Strong Fluorescence	
Water	HMX	TDG	DMMP	
Amino Acids	PETN	DIMP	TEPO	C4
Alcohols	RDX			Microbes
Aliphatics		Ammonia Nitrate	ANFOs	Toxins/Proteins
DNA/RNA	TNT	Urea Nitrate		Narcotics
Lipids	Perchlorates	Nitroglycerin		Aromatic Amino Acids
		Ketones/Aldehydes		

Figure 4. Overall relationship between the Raman and fluorescence information from weakly and strongly absorbing target material.

An additional advantage of using deep UV excitation is that because such a wide array of important target materials strongly absorb at these wavelengths, there is a natural spatial separation of superficial material from substrate or background material, which assists in discriminating the "topical" material from "deeper" material and provides a method of segregation of mixed materials.

Detection of materials with any analytical method requires a database of samples against which an unknown sample can be compared. To understand the effect of a changing parameter, e.g. spectral resolution or spectral range, one needs to "visualize" changes in the relationship between samples as a parameter is varied. Multivariate analyses offer a solution by reducing the dimensionality of the input data; isolating components that provide the greatest separation. Using an approach like principal component analysis (PCA), samples that are spectrally alike, will cluster together. The ability to differentiate materials using either Raman or fluorescence alone was discussed in the 2012 paper [1] in detail and will not be repeated here. However, the focused message is that chemometric analysis using Raman alone of 27 diverse samples shows major clustering based on ubiquitous C=C and C-H Raman bands which dominate the spectra of a wide range of organic materials and makes differentiation of these compounds difficult when using Raman alone. High spectral resolution Raman can alleviate this problem, but fluorescence spectra, even at low spectral resolution, clearly differentiates most of these organic compounds. This is illustrated in Fig. 5 below.

When chemical clustering occurs correctly, samples in one cluster should have some chemical commonality where nearby clusters should consist of samples with minor variations associated to small changes in the chemistry (i.e., the second order separation). If these changes are small, e.g., benzene versus a spore (containing dityrosine), these clusters should be closer than chemicals like benzene and anthracene (one ring versus 3 ring aromatics). In the case above, where aromaticity drives separation and a reduction in spectral range causes anthracene to closely cluster with benzene, these should never be nearby in chemometric space. In this case, the cluster containing anthracene can technically be a separate cluster.

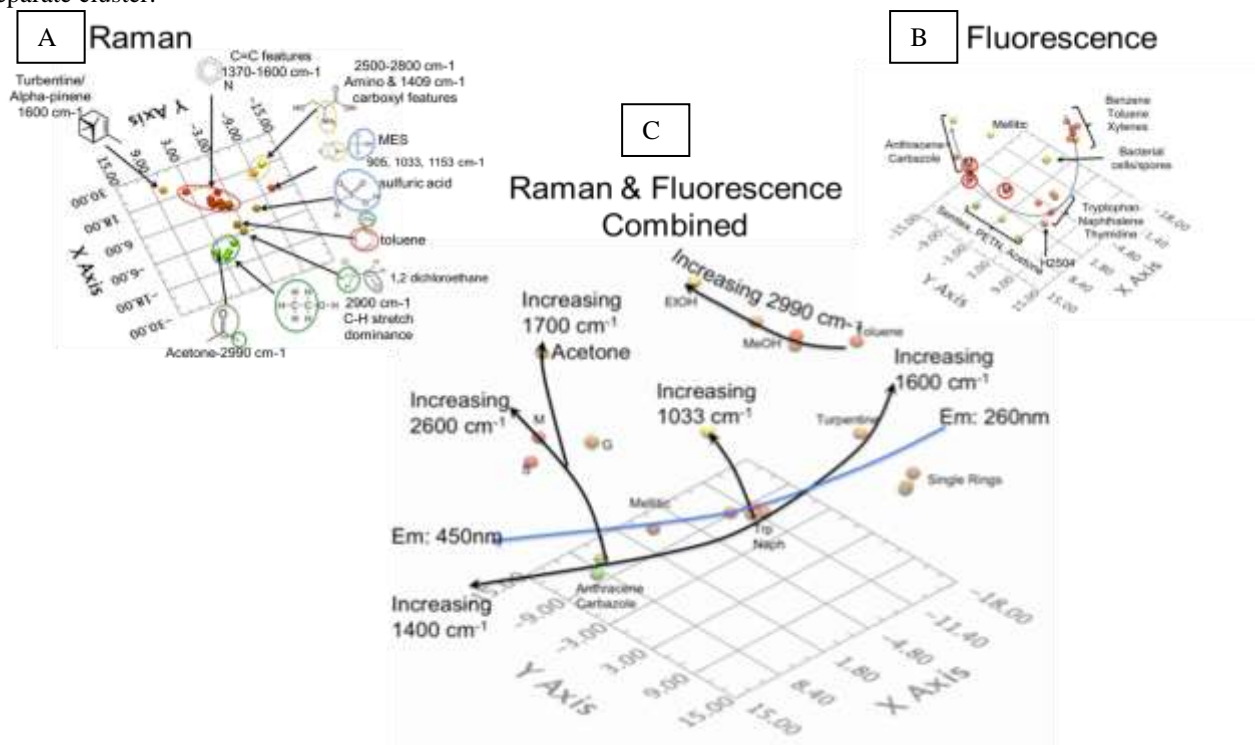
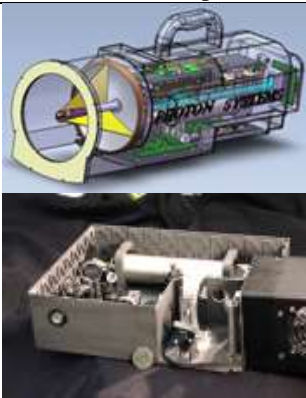


Figure 5. PCA analysis of 27 diverse samples using A) Raman alone, B) fluorescence alone, C) combined Raman & fluorescence.

Combining both Raman and fluorescence spectra in a common PCA analysis clearly separates different organic compounds into different groupings. In Fig. 5C, the trendlines indicate how the samples are separated. The blue line is the effect of the fluorescence information and sets the “backbone” of the chemometric space. The 1400 to 1600 cm⁻¹ Raman trendline closely follows this but causes some of the aromatic samples like turpentine to migrate away from the fluorescence trendline. The combination of low wavelength fluorescence and strong C-H stretching mode uniquely place toluene in the chemometric space. Xylenes however did not exhibit this C-H feature in its Raman spectrum. Therefore it clusters in the single ring group.

4. DEEP UV RAMAN & FLUORESCENCE INSTRUMENTS

The advantages of deep UV Raman spectroscopy alone and in combination with fluorescence spectroscopy have been demonstrated in many laboratory environments using large laboratory instruments. We do not provide an extensive literature here, but some literature is in the attached references. One of our goals is to bring this technology to handheld field operations with standoff distances from a few cm to 25 m. The focus of the data shown below will be for these miniature instruments, starting with a Targeted Ultraviolet CBE (TUCBE) chemical sensor and finishing with a next generation sensor with much higher spectral resolution for both Raman and fluorescence. We will also show some results on our laboratory based macroscopic chemical mapping instruments called MOSAIC instruments with a sensitivity to a single bacterial spore or ng/cm² of chemical, and microscopic chemical imaging instruments with sensitivity to a small fraction of the contents of a single bacterial spore. A selection of these instruments is shown below in Table I

			
	Handheld Standoff (TUCBE)	Macroscopic (MOSAIC)	Microscopic (μ MOSAIC)
Working distance	0.1-25 m	2-20 cm	1-10 mm
Spatial resolution	0.1-10 mm	50 – 500 μ m	150 – 200 nm
LOD	60 spores or low μ g/cm ² at 5 m	Single spore or ng/cm ² at 5 cm	Small fraction of single spore (live) or pg sample

Results from two different hand-held standoff instruments will be described: a low spectral resolution instrument called TUCBE 4.5, and a higher resolution instrument called SHERLOC. All systems employ a commercially available 248 nm NeCu laser with output of several hundred mW during pulse width about 40 μ s with pulse repetition rates typically up to about 40 Hz. This laser emits a relatively “soft” pulse on targets, providing little or no sample damage, even to delicate bacterial cells or spores. The top image in Table I under hand-held standoff instrument is a TUCBE 4.5. This instrument has an overall weight about 15 pounds including batteries for typical field operations of several days. It incorporates a 250 mm focal length Raman spectrometer and f/6.3 objective lens and has a spectral resolution about 80 cm⁻¹ using a 32-channel PMT array detector. It also has a simultaneous fluorescence spectrometer with six channels covering a range from 280 nm to 380 nm using single channel PMT detectors. As an example of the effect of spectral we employed high resolution spectra of 18 chemicals with excitation at 248 nm [12]

5. EFFECT OF RAMAN SPECTRAL RESOLUTION OF CHEMICAL DIFFERENTIABILITY

An example of the effect of Raman resolution on chemical specificity was illustrated by spectral binning of high resolution Raman spectra using data from Linda Bowerman and Arthur Sedlacek at Brookhaven National Laboratory (BNL) [12]. These spectra are shown in a single image below in Fig. 6.

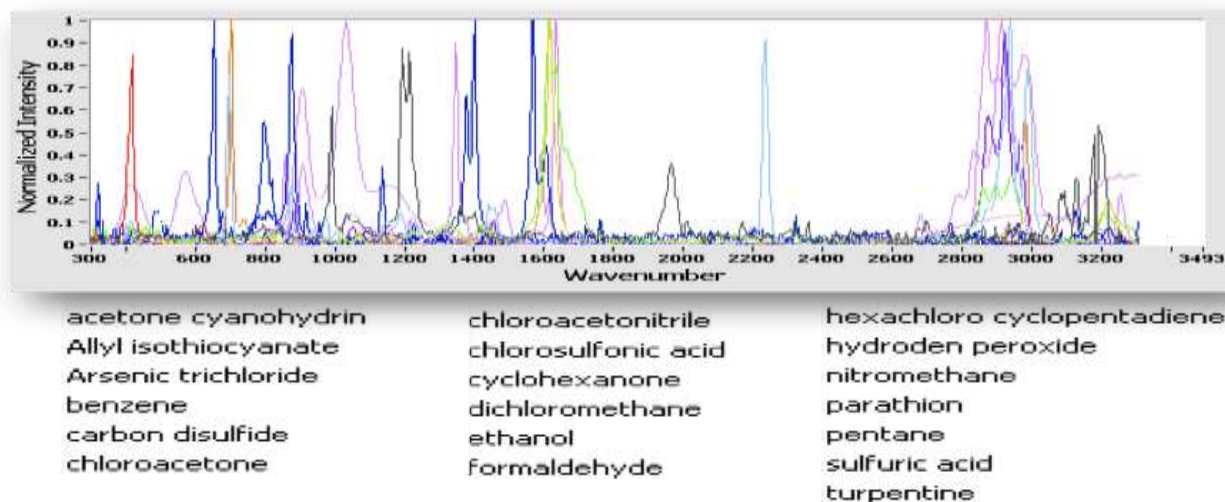


Figure 6. High resolution UV Raman spectra of toxic industrial chemicals with excitation at 248 nm [12]

We used PCA to observe chemical distinguishability or separation as it groups compounds by how similar their spectra co-vary. In contrast to the approach from the previous analysis where vector directions were used, we now visualize the mixing and movement of groups as a function of resolution. *The results show that groupings that are present with a spectral resolution of 3cm^{-1} remain intact up to a spectral resolution of 60cm^{-1} with minor variation at 80cm^{-1} .* The data presented in Figure 7 are from the BNL dataset and include spectral lines from $600\text{--}3300\text{cm}^{-1}$. We have denoted each group by color.

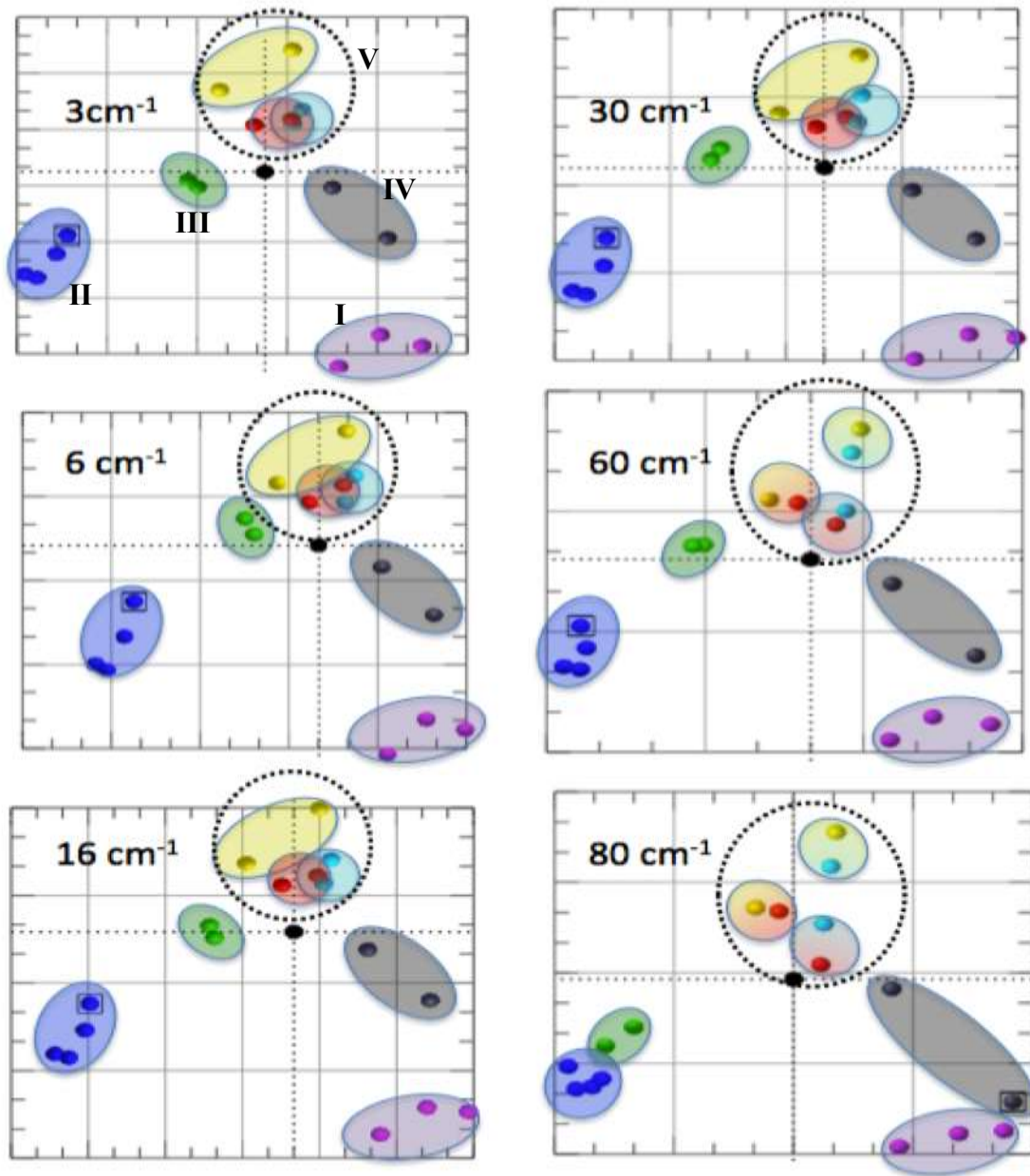


Figure 7. Chemical differentiability using DUV Raman spectra at 6 different resolution values with $E_x=248\text{ nm}$

There are 5 primary groups that are observed in Fig. 7, identified in the 3 cm^{-1} figure at top left by Roman numeral. Each group consists of compounds that co-vary when using the highest resolution data (3cm^{-1}). **Group I** are carbon based compounds containing a *ketone or terpene structures*. **Group II** primarily contains carbon-based compounds with *methyl or hydroxyl groups*. **Group III** consist of linear *carbon-chloride* compounds. **Group IV** consist of *single*

ring aromatic compounds. **Group V** consists of 3 subgroups that can be best described as *explosive or highly reactive materials* and include sulfur compounds, H_2O_2 , and nitromethane. Each group consists of compounds that co-vary when using the highest resolution data ($3cm^{-1}$). The purpose of this analysis was to not only to group compounds, but to watch these groups collapse as the spectral resolution is decreased. With a decrease in spectral resolution, the total variance between all compounds does decrease. However, the results suggest that separation of these compounds requires a spectral resolution no better than about $60 cm^{-1}$. Even at $80cm^{-1}$, only a few compounds begin to mix.

6. RESULTS FOR NEXT GENERATION HAND-HELD SENSOR

Based on the analysis described in Section 5 above, we began development of next generation sensors to improve the spectral resolution for both Raman and fluorescence emissions as well as to reduce the size and weight of the overall sensor package. A photograph of one version of this next generation sensor, called SHERLOC, is shown below in Fig. 8 as configured for mounting on a rover arm on NASA's 2020 Mars lander [11]. This instrument employs the same 248 nm laser used in the TUCBE 4.5 but a different optical system design, spectrometer, and different detector: a 3-stage thermoelectrically (TE) cooled, back thinned, back illuminated CCD array detector. The NeCu laser is the silver tubular item in the photo below. SHERLOC also has an autofocus lens with built-in raster scanner to enable deep UV Raman and fluorescence chemical imaging over an area about $1 cm^2$. SHERLOC is about $6'' \times 8'' \times 3''$ and weighs less than 9 pounds.

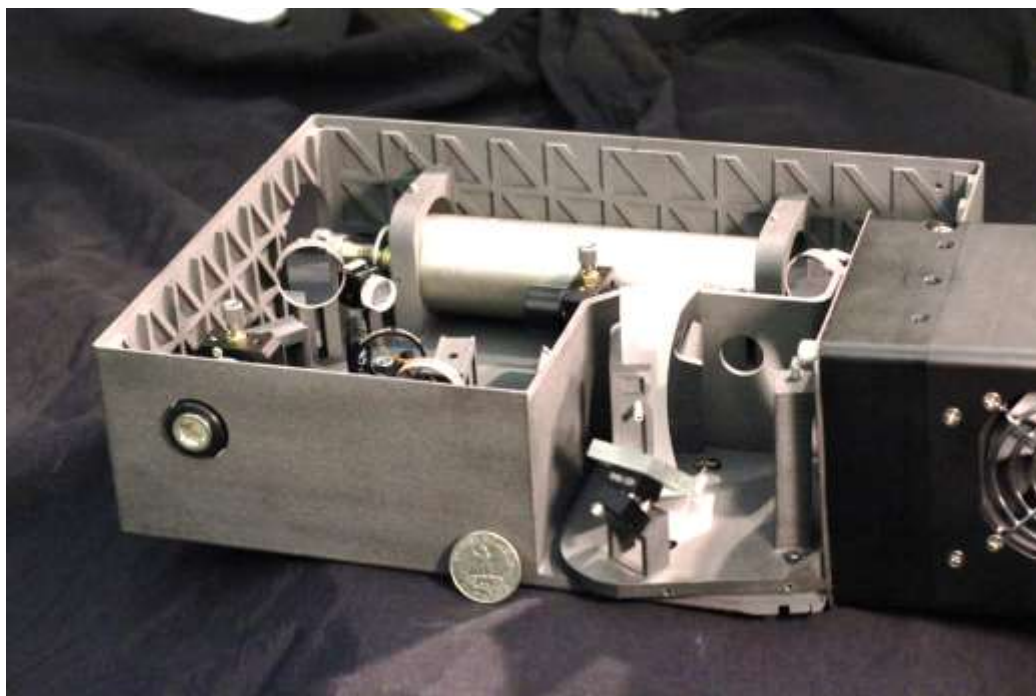


Figure 8. Photo of the SHERLOC, an instrument for deep UV Raman & fluorescence chemical imaging on Mars [11]. Approximate dimensions $6'' \times 8'' \times 3''$, less than 9 pounds for the complete sensor with laser, spectrometer, detector, autofocus mapper and all optics and electronics. A U.S. Quarter dollar is shown in the photo for size reference.

Raman and fluorescence spectral capabilities are illustrated in a series of figures below using the same miniature 248 nm NeCu laser as used in the TUCBE 4.5 sensor but combined with the 3-stage TE cooled CCD array detector rather than the 32- element PMT array detector. Figure 9 shows the raw Raman spectra of SEMTEX and its primary ingredients PETN and RDX without any baseline subtraction or compensation. Solar blind exposure time was about 10 seconds. SEMTEX has 76% PETN, 4.6% RDX, 9% plasticizers, and other more minor ingredients. The deep UV Raman spectrum of SEMTEX is different from the Raman spectra of its key ingredients, as seen in Fig. Some Raman bands of the major ingredient, PETN, are shifted, some enhanced, and some suppressed when combined with the other ingredients in SEMTEX. In all three spectra, the Raman band for nitrogen is seen at about $2350 cm^{-1}$ due to the air between the objective lens and samples tested.

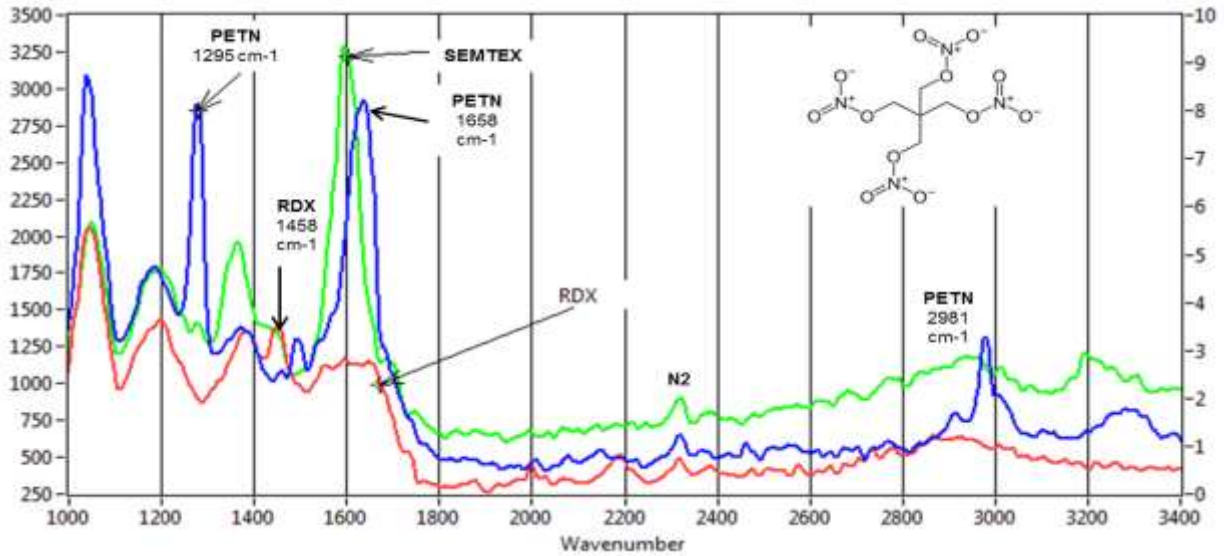


Figure 9. Raman spectra of SEMTEX and its major components PETN and RDX with excitation at 248 nm. Spectral data are raw with no baseline subtraction or compensation.

The fluorescence spectra of these same material plus a few more explosives is shown in Fig. 10. Like SEMTEX, C4 is a composite material made up of 91% RDX, 5.3% plasticizers, 2.1% binders, and other ingredients. PETN is a fundamental active explosive ingredient that has significant fluorescence emission below 400 nm although other active ingredients such as RDX and TNT show very little fluorescence signature. It should be noted that even weak fluorescence emissions are normally very strong compared to Raman emissions.

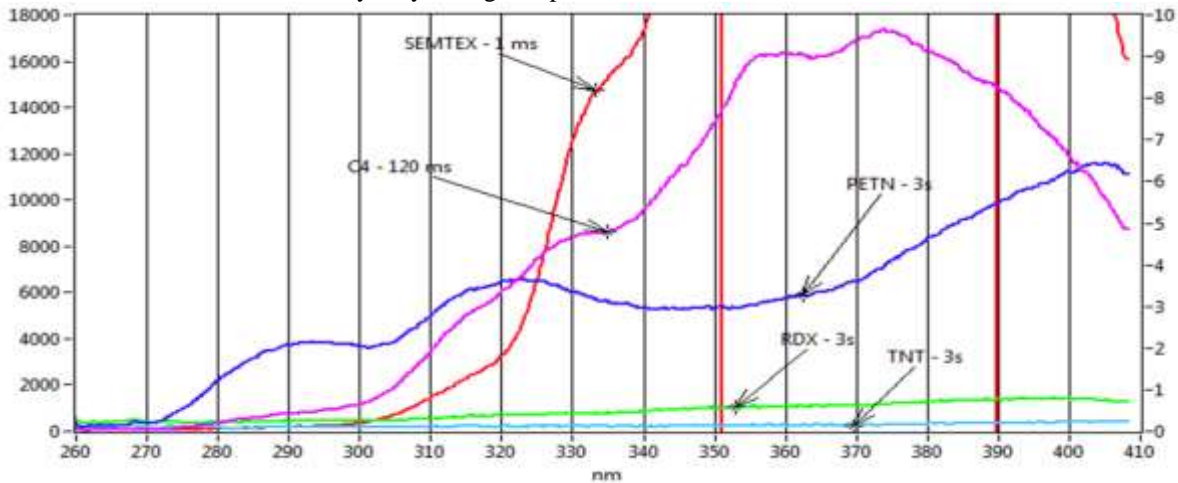


Figure 10. Fluorescence spectra of several composite explosives materials and their key ingredients. Spectral data are raw with no baseline subtraction or compensation.

Figure 11 shows the Raman spectra of C4 and its major ingredient, RDX. These spectra agree better than SEMTEX/PETN in Fig. 9 although it is believed that the RDX spectra had a truncated 1598 cm⁻¹ band due to location detection location on the sample. Again, the nitrogen band at 2350 cm⁻¹ from ambient air is present as well as features near 2200 cm⁻¹ and 2950 cm⁻¹. Some fluorescence background is seen starting to ramp up above about 2400 cm⁻¹, likely due to plasticizers, binders, etc. in the material.

The Raman spectrum of TNT is the final military grade explosive material shown below in Fig. 11. Again, there are very clear Raman features of this material. Not mentioned before is that two artifacts in the spectral data are the Raman

bands shown in Fi. 11 for SiO₂ near 1050 cm⁻¹ and 1200 cm⁻¹. This is due to the proximity of the explosives sample and fused silica slides, between which the samples were sandwiched.

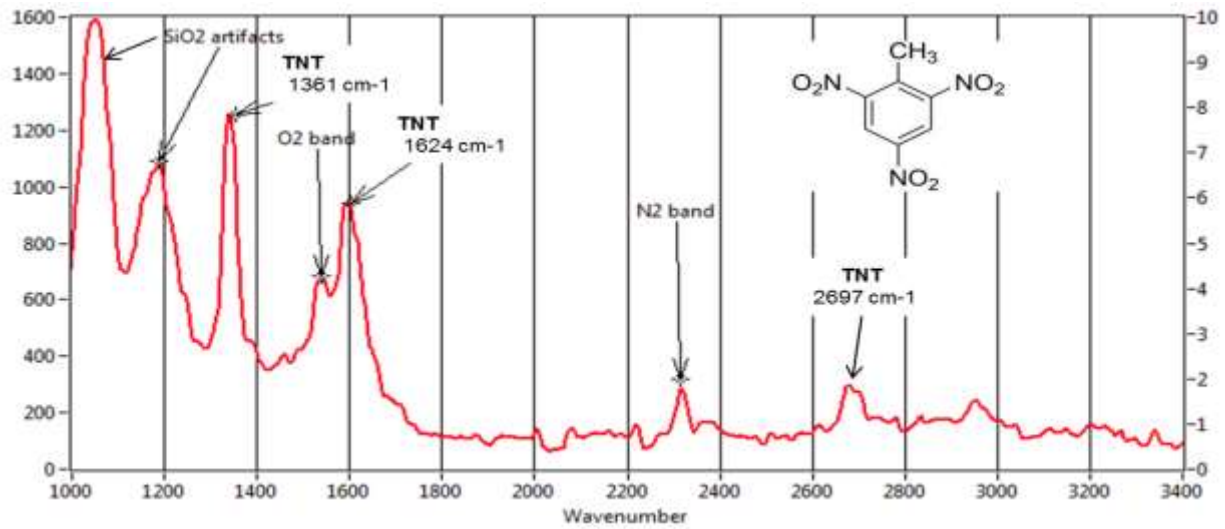


Figure 11. Raman spectra of TNT with excitation at 248 nm. Spectral data are raw with no baseline subtraction or compensation.

Figure 12 shows the Raman spectra of several common energetic material oxidizers including chlorates, perchlorates, sulfates plus one chemical agent analog, DMMP.

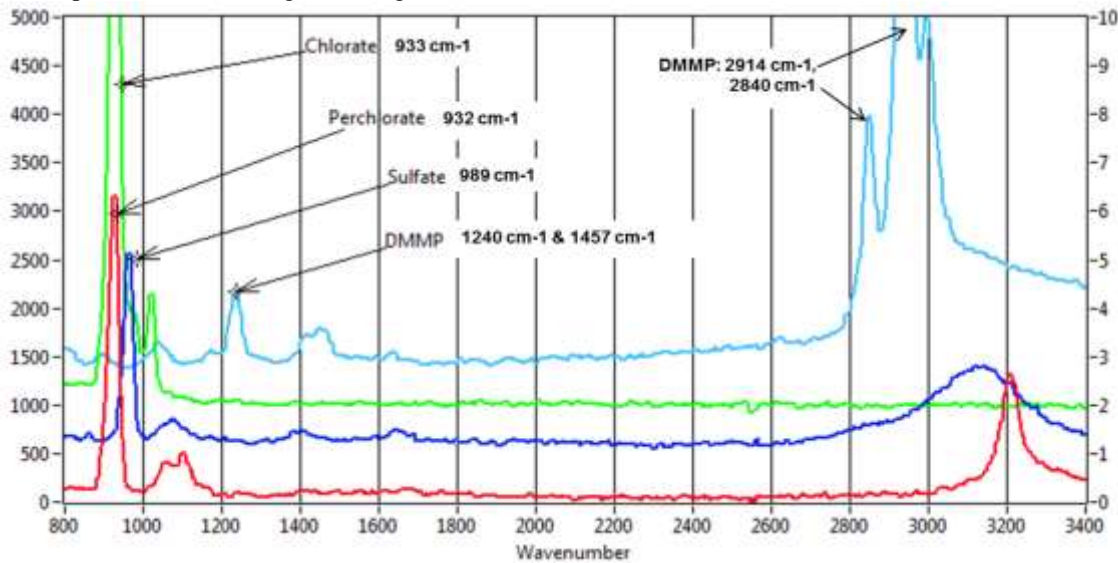


Figure 12. Raman spectra of several common oxidizers plus one chemical agent analog, DMMP with no baseline subtraction or compensation.

Figure 13 shows the fluorescence spectra of the nitrates, chlorates, perchlorates as well as carbonates, DMMP, and Ecoli to show the variability.

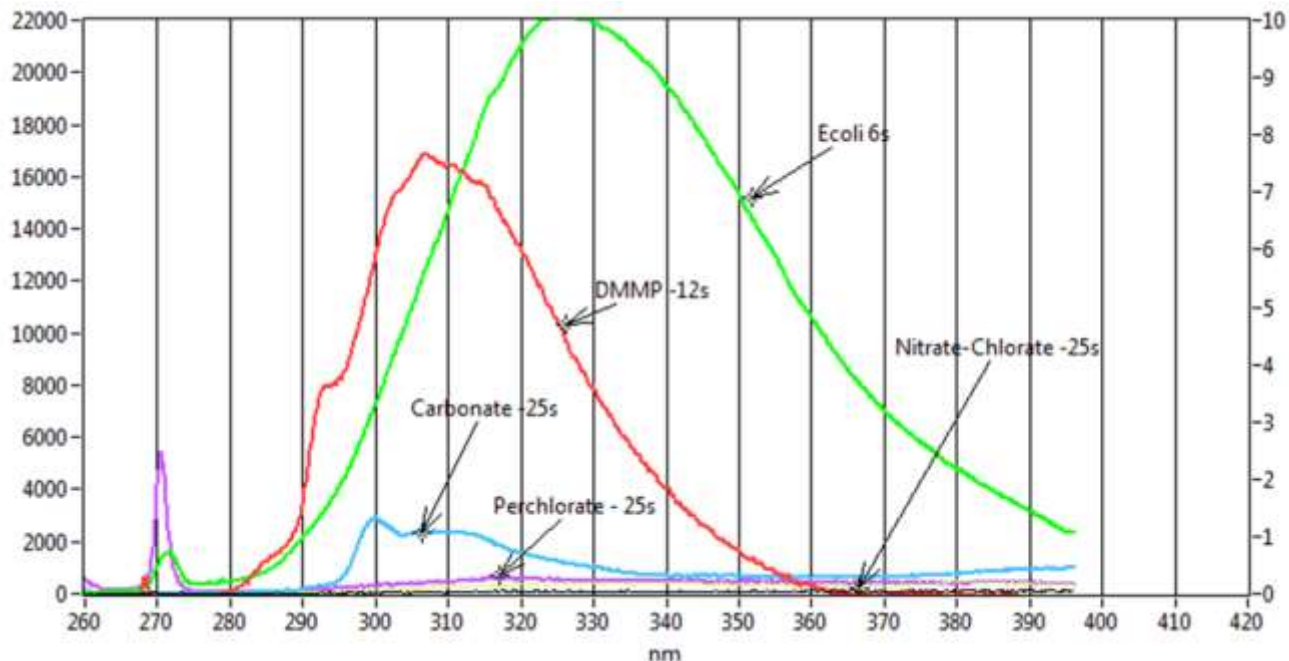


Figure 13. Fluorescence spectra of nitrates, chlorates, perchlorates, carbonates, DMMP, and Ecoli. Ex=248 nm

7. SUMMARY

These results show the advantages of deep UV excitation below 250 nm to enable fluorescence free Raman spectra of materials which contain fluorescence features either within the target material or in the surroundings, within the laser excitation spot. These results also demonstrate that Raman and fluorescence emissions occur in distinct spectral regions when excitation occurs below 250 nm. This enables simultaneous and solar blind detection of both orthogonal forms of emission from unknown samples and improves sensing by increasing the probability of detection and reducing the probability of false detection.

These results also demonstrate the ability to obtain both Raman and fluorescence spectra from a wide range of materials using existing commercial lasers and detectors in a fully integrated sensor weighing less than 10 lbs with dimensions less than about 6"x8"x3", compatible with hand-held or small arm mounted robotic operations. Normal concept of operations uses the high sensitivity and relatively lower specificity of fluorescence to rapidly interrogate and area to look for features of interest, followed by Raman spectroscopy to provide confirmation and/or further elucidation of target material identity.

8. ACKNOWLEDGEMENTS

Photon Systems gratefully acknowledges the support of: U.S. Army STTR Contract No. W911SR-11-C-0089 under the program management of Dr. Augustus W. Fountain, and Dr. Steven Christesen; DTRA Contract No. HDTRA1-09-C-0010 under the program management of Dr. Timothy Leong; and NASA Astrobiology Science & Technology Instrument Development (ASTID) Contract No. NNH10ZDA001N.

9. REFERENCES

- [1] Bhartia, R., W. F. Hug, and R.D. Reid, "Improved sensing using simultaneous deep UV Raman and fluorescence detection", SPIE Security & Defense, Vol. 8358, No. 46, April 26, 2012.
- [2] Asher, S.A., and C.R. Johnson, "Raman Spectroscopy of a Coal Liquid Shows That Fluorescence Interference Is Minimized with Ultraviolet Excitation", Science, 225, 311-313, 20 July (1984).
- [3] Asher, S.A. and C.R. Johnson, "UV Resonance Raman Excitation Profile Through the 1B_2 State of Benzene", J. Phys. Chem. Vol. 89, pp. 1375-1379 (1985).
- [4] Nelson, W.H., R. Manoharan and J.F. Sperry, "UV Resonance Raman Studies of Bacteria", App. Spect. Reviews, 27 (1), pp67-124, (1992)

- [5] Sparrow, M.C., J.F. Jackovitz, C.H. Munro, W.F. Hug, and S.A. Asher, "A New 224nm Hollow Cathode UV Laser Raman Spectrometer", *App. Spect.*, Vol. 55, No. 1, Jan (2001).
- [6] Wu, M., M.Ray, K.H.Fung, M.W. Ruckman, D. Harder, and A.J. Sedlacek, "Stand-off Detection of Chemicals by UV Raman Spectroscopy", *App. Spect.*, Vol.54, No.6, pp. 800-806 (2000).
- [7] Christesen, S.D. et al. *J. Appl Spec.* 62(10):1078-83, Oct., (2008)
- [8] Hug, W.F., R. Bhartia, A. Tsapin, A. Lane, P. Conrad, K. Sijapati, and R. D. Reid, "Water & surface contamination monitoring using deep UV laser induced native fluorescence and Raman spectroscopy", *Proc. SPIE*, Vol. 6378, Boston, MA. Oct. (2006).
- [9] Hug, W.F., R.D. Reid, R.Bhartia, and A.L.Lane, "Status of Deep UV Lasers for UV Resonance Raman and Native Fluorescence CBE Sensors", Invited Speaker, Conference on Lasers and Electro-Optics, PhAST 2, May 10, 2007
- [10] Bhartia, R., W.Hug, E.Salas, R.Reid, K.Sijapati, A.Tsapin, W.Abbey, P.Conrad, K.Nealson, and A. Lane. "Classification of Organic and Biological materials with Deep UV Excitation", *Applied Spectroscopy*, Vol. 62, No. 10, October 2008.
- [11] Beegle, L.W., R. Bhartia, W. Hug, et.al., "SHERLOC: Scanning Habitable Environments with Raman and Luminescence for Organics and Chemicals", 45th Lunar & Planetary Science Conference, p. 2835, Houston, TX, 2014
- [12] Linda Bowerman and Arthur Sedlacek, "Ultraviolet Raman Spectral Signature Acquisition-III, ITT Year-End-Report, FY2004, Rev. 9.